JOURNAL OF GUIDANCE, CONTROL, AND DYNAMICS
Vol. 18, No. 1, January–February 1995

Case Study on Haptic Devices: Human-Induced Instability in Powered Hand Controllers

H. Kazerooni* and Tanya J. Snyder*
University of California, Berkeley, Berkeley, California 94720

This article describes the dynamic behavior of a hand controller when it is maneuvered by a human. A general control architecture is developed that guarantees various impedance's on the hand controller. We show that some compliancy either in the hand controller or in the human arm is necessary to achieve stability of the hand controller and the human arm taken as a whole. The actuators' backdrivability, the dynamics of the hand controller mechanisms, and the computer sampling time are discussed as they relate to system stability. A set of experiments that were performed on a prototype hand controller are presented to show the system performance.

Nomenclature

The Laplace argument s for all functions will be omitted throughout this article except when new quantities are defined or when required for clarity.

$e(s)$ = input command to hand controller, s is Laplace variable
$f(s)$ = force on hand controller
$G(s)$ = hand controller dynamics with positioning controller
$H(s)$ = human arm dynamics
K_0 = DC gain of $K(s)$
$K(s)$ = compensator (operating on contact force f)
m = force imposed by human muscles
$P(s)$ = dynamics of hand controller mechanism
$S(s)$ = sensitivity function of hand controller
$x(s)$ = hand controller position
τ = time constant of $K(s)$

I. Introduction

POWERED hand controllers are active multi-degree-of-freedom joystick-like haptic devices that are maneuvered by humans to generate commands. For example, powered hand controllers can be used as force-reflecting master robots in telerobotic systems. They can also be used by helicopter pilots for commanding pitch and roll. In another application, an operator aboard a mother ship uses a hand controller to maneuver an unmanned underwater vehicle. Figure 1 shows a multi-degree-of-freedom hand controller being maneuvered by a human. Hand controllers should be discriminated from controllers that consist of multiple levers and switches, with each lever corresponding to an individual axis. Instead, a hand controller allows commands related to multiple degrees of freedom to be integrated into a single hand movement. The novelty of a hand controller is apparent in the example of maneuvering an unmanned underwater vehicle. (Traditionally, the speed of the underwater vehicle in various directions is a function of the position of the hand controller in various directions.) The operator can control the three-dimensional motion of the vehicle using a single handgrip.

Hand controllers fall into two categories: passive and active. Passive hand controllers are unpowered and do not provide any force feedback to the operator. The passive hand controller consists of linkages, encoders, and other passive elements. Some passive hand controllers also include springs and dampers in the joints to provide resistance to motion. Lippay et al.[1] describe a multi-degree-of-freedom passive hand controller used for helicopter flight control. Glusman et al.[2] formulate a helicopter handling quality using a multi-degree-of-freedom passive hand controller. A fundamental limitation in the performance of a passive hand controller arises from one's inability to modulate the dynamic behavior of the hand controller. This is true because the passive hand controller's behavior is a fixed function of the dynamics of the mechanism hardware. Active hand controllers, however, include powered actuators in the mechanism joints as well as force sensors. The actuator at each joint is used to produce an arbitrary resistance to the operator's motion. This resistance to motion can be modulated by a computer to provide different dynamics for different axes. For example, pilots usually prefer to feel a high stiffness in the pitch motion and a low stiffness in the roll motion. In another example, the hand controller may have to be rolled and pitched along arcs that have significantly different radii. Note that the axes of the coordinate frame for a desired dynamic behavior (impedances) do not, in general, coincide with the hand controller's motor axes these; desired impedances must be developed electronically by a computer. See Refs. 3 and 4 for descriptions of novel powered hand controllers.

Powered hand controller's are of paramount importance in force-reflecting telerobotic systems.[5–8] In these systems, the hand controller's resistance to motion is a function of the forces applied to the controlled machine. For example, while maneuvering an unmanned underwater vehicle with a force-reflecting hand controller, the position of the hand controller would correspond to the velocity of the vehicle, whereas the force on the hand controller would correspond to the drag forces on the vehicle. In another example, a force-reflecting hand controller is the master in a master-slave telerobotic system. "Telepresence" denotes a dynamic behavior in a telerobotic system in which environmental effects experienced by the slave are transferred through the master to the operator without alteration; therefore, the human feels that he or she is "there" without "being" there. See Refs. 9 and 10 for the role of force reflection in telemanipulations.

This article is concerned with the stability of a powered hand controller interacting with a human arm. (See Ref. 5 where the stability of a more complicated system—human arm holding on a hand controller and a slave robot interacting with an environment—has been described.) In particular, the following topics are discussed in this paper.

1) Theoretical derivation of a control law that ensures stability for a limited range of hand controller impedances is considered.

2) Derivation of the tradeoffs between the achievable bandwidth and the desired impedance is discussed; one cannot choose an arbitrarily soft impedance for the hand controller and still achieve a wide bandwidth.

Section II describes the hand controller and human arm dynamic behavior. Section III introduces the control architecture. Section IV derives a stability condition. Section V provides suggestions for

Received May 18, 1992; revision received March 17, 1994; accepted for publication May 25, 1994.

*Mechanical Engineering Department.

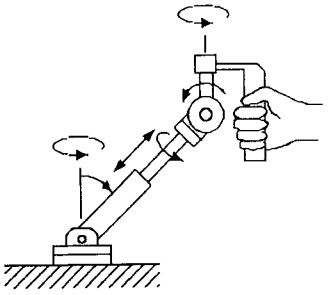

Fig. 1 Schematic of a six-degree-of-freedom hand controller.

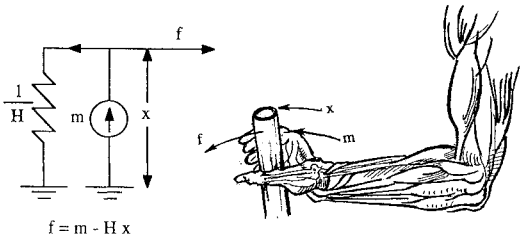

Fig. 2 In constrained movements, contact force f is a function of not only m but also imposed position constraint x. In a Norton equivalent circuit current f is a function of not only the current source m but also of the imposed voltage drop x.

preventing instability, and finally Sec. VI describes the trade-offs between stability and performance via a set of experiments.

II. Modeling

This section models the dynamic behavior of the hand controller and the human arm. We represent the hand controller and the human with general unstructured models. Since these models are unstructured, they encompass a wide variety of hand controller and human arm dynamic behavior. Although this modeling approach may not lead to a particular design procedure, it will enable us to understand the fundamental issues involved in the stability of a system consisting of a hand controller and human arm.

A. Hand Controller

The hand controller is assumed to have a closed-loop position controller. A closed-loop position control system minimizes the effects of frictional forces in the joints and in the transmission mechanism and creates a more definite dynamic behavior in the mechanism. Minimizing the effects of uncertainty in electromechanical systems is a common design specification for position controllers. (See Ref. 11 for a design method.) A closed-loop position control system creates linear dynamic behavior in the hand controller. It is assumed that, for nonlinear hand controller dynamics, a nonlinear stabilizing controller has been designed to yield a nearly linear closed-loop position system for the hand controller. This allows us to assume that the hand controller closed-loop dynamics can be approximated by transfer functions.

The endpoint position of the hand controller is a dynamic function of both its input command e and the human force f. The structure of the positioning controller is not of importance in this analysis. Here G and S are two transfer functions that relate the hand controller endpoint position x to the input command e and the human force f:

$$x = Ge + Sf \tag{1}$$

The motion of the hand controller endpoint in response to imposed forces f is caused by either structural compliance in the hand controller or the compliance of the positioning controller. The sensitivity function S maps the forces due to human contact to the hand controller position. Whenever a contact force is applied to the hand controller, the endpoint of the hand controller will move in response. If the hand controller has a "good" positioning controller, the change in position due to the contact force will be "small" as long as the magnitude of the contact force lies within certain limits. Note that G and S depend on the nature of the closed-loop controller. If a compensator with several integrators is chosen to ensure small steady-state errors, then S will be small in comparison to G. If the hand controller actuators are non-backdrivable, then S will be small regardless of the structure of the hand controller's positioning compensator. (Throughout this paper, we analyze hand controller and human arm dynamics using unstructured dynamic models that focus on the input-output relationships rather than a particular dynamic structure. The framework of unstructured models leads to general conclusions; however, a given hand controller's dynamics are typically characterized by a structured model.)

B. Human Arm Dynamics

Human arm maneuvers fall into two categories: constrained and unconstrained. In a constrained maneuver, the human arm is in contact with an object continuously, whereas in an unconstrained maneuver, the human arm is not in contact with anything. Since the human arm is always holding the hand controller during a maneuver, our primary focus is on constrained maneuvers of the human arm. The dynamic behavior of the human arm's constrained, single-joint movements is modeled as a functional relationship between a set of inputs and a set of outputs. As a specific example, the joint being modeled may be the elbow joint, actuated by the elbow flexor (biceps) and the elbow extensor (triceps). We avoid attributing a particular class of dynamic behaviors to constrained movements of the human arm, as it is not clear whether the arm behaves as a force or a position control system in constrained motions. Maneuvering our hands in a stream of water from one point to another target point while struggling with the water current is an example that shows the human arm can work as a position control in a constrained space and can continuously accept a position or velocity command from the central nervous system. Alternatively, pushing a pin into a wall is an example of a constrained movement where the human imposes a force on the pin without being concerned with the pin position in the direction normal to the wall; this system may be viewed as one that accepts force commands from the central nervous system. Considering the above dilemma in attributing a particular control action to constrained movements of the human arm, we use a Norton or a Thevenin equivalent concept to arrive at a general substitute for the dynamic behavior of the human arm interacting with the hand controller. In the same way that the choice of a Norton or Thevenin equivalent does not affect the behavior of a circuit in contact with other circuits, our choice in modeling the human arm by a Norton or a Thevenin equivalent has no effect on the arm's interaction with other systems. Using the "force-current" analogy between electrical and mechanical systems, a Norton equivalent is now chosen to model the human arm's dynamic behavior as a nonideal source of force interacting with the hand controller. The notion of "nonideal," as applied here, refers to the fact that the human arm responds not only to descending commands from the central nervous system but also to position constraints imposed by interaction with the hand controller.

The term m is the part of the contact force that is imposed by the muscles, as commanded by the central nervous system. If the human arm does not move (i.e., the arm position $x = 0$), the total contact force f is the same as m. However, f is also a function of the hand controller position constraint. If the arm moves (i.e., the hand controller imposes a position constraint on the human arm), the force imposed on the hand controller will differ from m. The analogy can be observed from the Norton equivalent circuit shown in Fig. 2: The current f is a function of not only the current source m but also the external voltage x. Considering the above analogy, shown in Fig. 2, the contact force f can be represented by

$$f = m - Hx \tag{2}$$

Throughout this article, H is referred to as the human arm impedance and maps the hand controller position constraint onto the contact force. The value of H is determined primarily by the physical and neural properties of the human arm. It will become clear later that H plays an important role in the stability and performance of the system; we will arrive at some experimental values for H in later sections. This model is in agreement with the modeling described

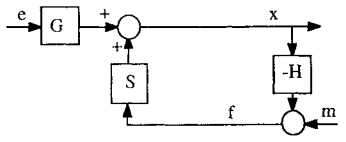

Fig. 3 Block diagram of hand controller and human arm.

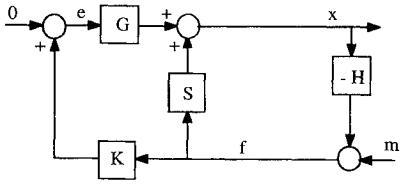

Fig. 4 Addition of force compensator to hand controller.

in Refs. 12 and 13. Figure 3 depicts how the hand controller and human interact dynamically.

III. Control Architecture

When the hand controller is not in contact with the human, the actual position of the hand controller endpoint is governed by Eq. (1), where $f = 0$. The feedback loop on the contact force f closes naturally when the hand controller encounters the human arm. Physical contact between the human and the hand controller produces some hand controller motion as f acts through S. In general, S is small. Thus, the human operator alone does not have sufficient strength to move the hand controller as desired. Figure 4 shows the system when a force compensator is incorporated in the control structure. Examining Fig. 4 reveals that K provides an additional path for f to map to x if K is chosen to be nonzero. The term K can be thought of as the component that shapes the overall mapping of the force f to the position x. This leads to an effective sensitivity of $S + GK$. (For brevity, we refer to the SH loop as the natural loop and the GKH loop as the compliance loop because it contains the compliance compensator K.)

The parameters G and S are determined by the mechanical design of the hand controller and by the chosen position controller. However, the designer has some freedom (limited by stability considerations) to adjust the effective sensitivity $(S + GK)$ along the path from f to x; $S + GK$ affects how the hand controller "feels" to the human operator. For instance, if K is chosen so $S + GK$ is approximately a constant, the hand controller reacts like a spring in response to f. Similarly, if $S + GK$ is approximately a single or double integrator, the hand controller acts like a damper or mass, respectively. A large value for K develops a compliant hand controller whereas a small K generates a stiff hand controller. One cannot choose arbitrarily large values for K; the stability of the closed-loop system of Fig. 4 must also be guaranteed.

IV. Closed-Loop Stability Condition

The Nyquist theorem is used to develop a sufficient stability condition for the closed-loop system in Fig. 4. This sufficient condition results in a class of compensator K that guarantees the stability of the closed-loop system. Note that the stability condition derived in this section does not give any indication of system performance but only ensures a stable system. Also, note that the stability condition is a sufficient condition, not a necessary condition.

An assumption is made that the system in Fig. 4 is stable when $K = 0$. The plan is to determine how robust the system is when the term GKH is added to the feedback loop. Note that there are two elements in the feedback loop: SH represents the natural feedback loop that occurs as a result of the interaction between the human arm and the hand controller whereas GKH represents the controlled compliance feedback loop. If the controller in the compliance feedback loop is eliminated by setting $K = 0$, the system reduces to the case where a human is manipulating the hand controller but the command input to the hand controller closed-loop position system is zero. The goal is to obtain a sufficient stability condition when K is added to the system. To achieve this, the Nyquist criterion[14] is used. The following assumptions are made:

1) The closed-loop system in Fig. 4 is stable when $K = 0$. It is assumed that the system remains stable when the human and the hand controller are in contact and no feedback is used in the system.

2) Here K is chosen as a stable linear transfer function. Therefore the loop transfer function $SH + GKH$ has the same number of right half-plane poles as SH. For convenience, in the stability analysis we assume $A = SH$ and $B = SH + GKH$.

According to the Nyquist criterion, the system shown in Fig. 4 remains stable as long as the number of counterclockwise encirclements of B around the origin of the s plane is equal to the number of unstable poles of the loop transfer function B. By assumptions 1 and 2, A and B have the same number of unstable poles. Assuming that the system is stable when $K = 0$, the number of encirclements of the origin by $1 + A$ is equal to the number of unstable poles in A. When compensator K is added to the system, the number of encirclements of the origin by $1 + B$ must be equal to the number of unstable poles in B in order to guarantee closed-loop stability. Because of the assumption that the number of unstable poles in A and B are identical, $1 + B$ must have exactly the same number of encirclements of the origin as $1 + A$. In order to guarantee equal encirclements by $1 + B$ and $1 + A$, insurance is needed that $1 + B$ does not pass through the origin of the s plane for all frequencies:

$$|1 + SH + GKH| \neq 0 \qquad \forall \omega \in (0, \infty) \tag{3}$$

A more conservative condition can be written as

$$|GKH| < |1 + SH| \qquad \forall \omega \in (0, \infty) \tag{4}$$

or

$$|GK| < |S + 1/H| \qquad \forall \omega \in (0, \infty) \tag{5}$$

Inequalities (4) and (5) express the stability condition of the closed-loop system in Fig. 4. [A less conservative stability condition to guarantee inequality states that the angle of $GHK + SH < 180$ $\forall \omega \in (0, \infty)$ whenever $|GHK + SH| = 1$. This inequality states that guaranteeing stability of the closed-loop system requires selecting K such that the phase margin for the loop gain of $GHK + SH$ is positive.] Inspection of inequalities (4) and (5) show that the smaller the sensitivity of the hand controller, the smaller K must be. Also from inequality (5), the more rigid the human arm is, the smaller K must be. In the "limiting case" when the hand controller is infinitely stiff $(S = 0)$ no K can be found to enable interaction with an infinitely rigid human arm (i.e., $H \Rightarrow \infty$). In other words, for stability of the system shown in Fig. 4, there must be some compliancy either in the hand controller or in the human arm. The hand controller compliancy may be due to structural flexibility and/or the electronic compliancy resulting from the positioning controller.

The stability condition for multi-degree-of-freedom systems (when G, K, H, and S are transfer function matrices) can be derived in a similar way using singular values:

$$\sigma_{\max}(GKH) < \sigma_{\min}(I + SH) \qquad \forall \omega \in (0, \infty) \tag{6}$$

The next section makes some suggestions for increasing the system stability range.

V. Suggestions for Increasing Stability Range

A. Increasing Sensitivity Function

Transmission systems with large transmission ratios that are not backdrivable result in small sensitivity functions S. We suggest that the hand controllers be designed such that they can be backdriven. This can be done by employing low-ratio transmission systems to drive the hand controller. Direct-drive systems, because of the elimination of the transmission systems, can potentially have a large S.

Another way to increase S is to decrease the position controller gain. The decrease in the position control gain may result in a sluggish response for the hand controller. However, we suggest that this gain be chosen as small as possible. In particular, we recommend that integral control be avoided in the position control loop. Integrators in the position loop result in a very small S, even when backdrivable actuators are used.

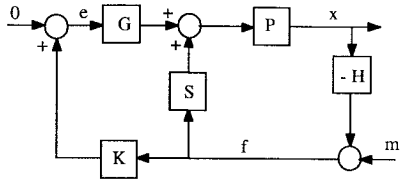

Fig. 5 Addition of mechanism dynamics *P*.

B. Mechanism Dynamics

The more rigid the structure of the hand controller, the wider is the achievable bandwidth of G. A hand controller, which has too many mechanical elements bolted together, will have dynamics that cannot be modeled correctly. If the hand controller mechanism is very rigid, then the block diagram of Fig. 4 is correct. However, if the mechanism contains a significant amount of unmodeled dynamics, the block diagram of Fig. 5 is more appropriate. Here P represents the structural dynamics associated with the flexibilities in the hand controller mechanism.

Note that loop SH is not an "information" loop; it is "power" loop. This loop shows how the human force affects the hand controller. The force imposed by the human may have frequency components that will excite the unmodeled structural modes of the systems represented by P, creating forces that will be read by the force sensor.

Using the Nyquist stability criteria, the stability condition in Fig. 5 is given by

$$|GK| < |S + 1/HP| \qquad \forall\omega \in (0, \infty) \tag{7}$$

Here P can become large at various frequencies due to the dynamics of the mechanism structure and drive train. If P is large and S is small, inequality (7) cannot be satisfied. To minimize the unmodeled dynamics, we suggest that the mechanism be designed with a minimum number of very light and rigid components. Also, K should be a low-pass filter. Our previous experiments[15] have shown that a 5-H bandwidth for K is sufficient for most maneuvers. One suggested form of K is given by

$$K = (K_0/\tau s + 1) \tag{8}$$

C. Effect of a Large Sampling Time

The GHK loop is a digital loop representing the information signal through the computer, and the SH loop is a continuous signal representing the power transfer to the hand controller. The computer sampling time affects only the GHK loop.

The computer sampling time determines how quickly forces sensed at the hand controller are converted to position commands. Our experiments show that, since a slow computer creates a large delay between the input force and the hand controller response, human force builds up on the hand controller. This large force is then read by the force sensor, which results in movement of the hand controller with such a large velocity that it pulls the human arm forward. This reverses the direction of the contact force f. The hand controller responds to this reverse force with a large velocity that pushes the human arm backward. This periodic motion (limit cycle instability) occurs in a very short amount of time, and the motion of the hand controller becomes oscillatory. This limit cycle instability can be analyzed using describing function analysis. We suggest the use of a computer fast enough that the sampling time can be made very small.

VI. Experiment

Figure 6 shows the experimental one-degree-of-freedom electrically powered hand controller. The operator's hand grasps a handle mounted on a piezoelectric force sensor. A harmonic drive is installed between the DC motor and the handle to transfer power to the handle. An encoder measures the orientation of the handle. A microcomputer is used for data acquisition and control.

Using the encoders for feedback, a primary stabilizing controller for the hand controller was designed to yield the widest bandwidth for the closed-loop position transfer function G and yet guarantee

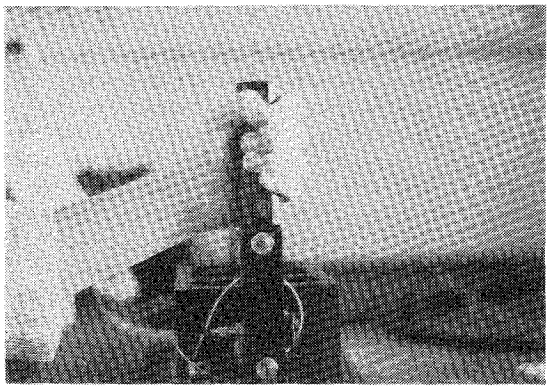

Fig. 6 One-degree-of-freedom hand controller.

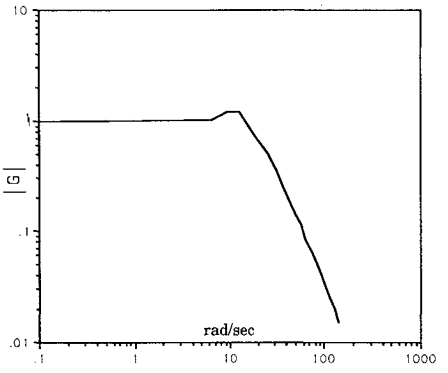

Fig. 7 A closed-loop position controller has been designed for a hand controller that minimizes effects of frictional forces in joints and in transmission mechanism and that creates more definite dynamic behavior in mechanism.

the stability of the closed-loop positioning system in the presence of bounded unmodeled dynamics in the hand controller and harmonic drive. The development of the position controller for the hand controller has been omitted for brevity. An experimental plot of G with a bandwidth of 10 rad/s is given in Fig. 7.

A human arm model was derived to verify the stability condition. The model derived for the human arm does not represent the human arm sensitivity H for all configurations of the arm; it is only an approximate and experimentally verified model of the author's arm in the neighborhood of the configuration shown in Fig. 6. For the experiment, the author gripped the handle, and the hand controller was commanded to oscillate via sinusoidal functions. At each oscillation frequency, the operator tried to move his or her hand to follow the hand controller so that zero contact force was maintained between the human hand and the hand controller. Since the human arm cannot keep up with highfrequency motion of the hand controller when trying to maintain zero contact forces, large contact forces and, consequently, a large H are expected at high frequencies. Since this force is equal to the product of the hand controller acceleration and human arm inertia (Newton's second law), at least a second-order transfer function is expected for H at high frequencies. On the other hand, at low frequencies (in particular at DC), since the operator can follow the hand controller motion comfortably, he or she can always establish virtually constant contact forces between the human hand and the hand controller. This leads to the assumption of a constant transfer function for H at low frequencies where contact forces are small for all values of hand controller position. Based on several experiments, at various frequencies, the best estimates for the author's hand sensitivity is presented by

$$H = \left(\frac{s^2}{20} + \frac{s}{5} + \frac{1}{5}\right) \text{lbf-ft/rad} \tag{9}$$

Figure 8 shows the experimental values and the fitted transfer functions [Eq. (9)] for the human arm dynamic behavior.

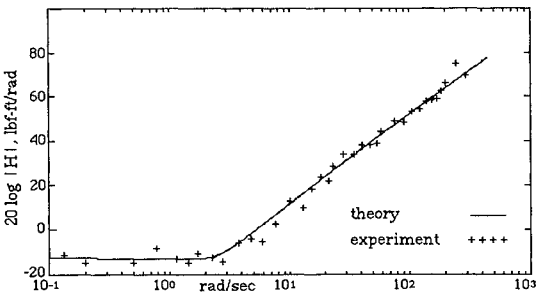

Fig. 8 Human arm dynamic behavior in the neighborhood of the configuration shown in Fig. 6.

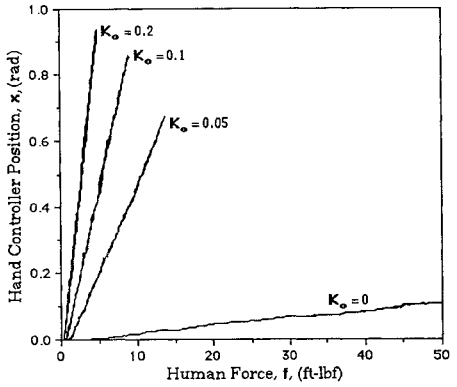

Fig. 9 By choosing K, the hand controller sensitivity function $S + GK$ can be shaped as desired. The larger K_0 (DC gain of K) is chosen to be, the more sensitive the hand controller will be in response to human forces.

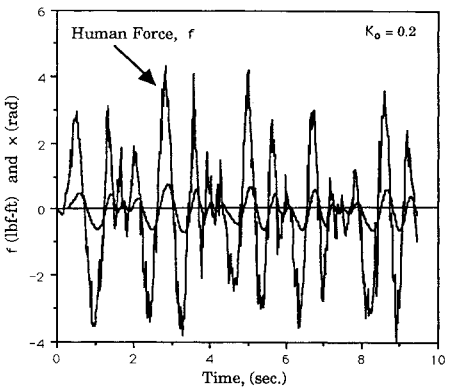

Fig. 10 Time history of human force f and hand controller position.

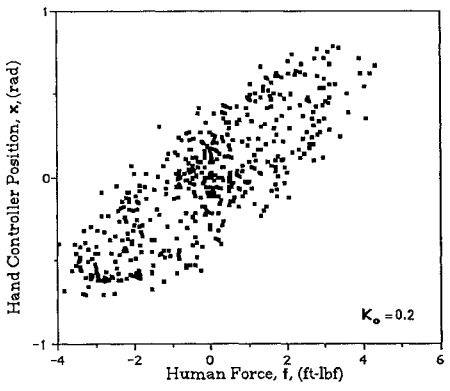

Fig. 11 Average slope of 0.2 reveals that $x = 0.2f$ for all frequencies within system bandwidth.

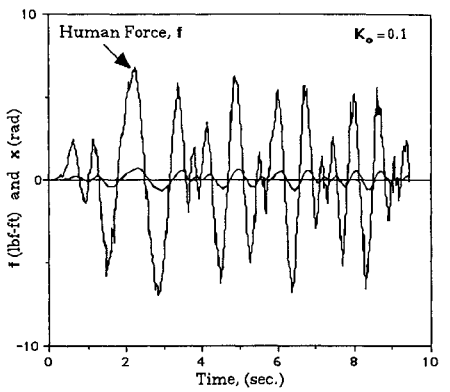

Fig. 12 Time history of human force f and hand controller position x.

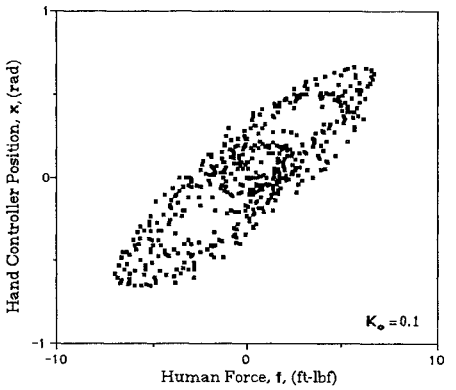

Fig. 13 Average slope of 0.1 reveals that $x = 0.1f$ for all frequencies within system bandwidth.

A. Performance with Low-Frequency Maneuvers

A set of experiments were performed to show how the hand controller sensitivity can be shaped. In particular the objective was to make the hand controller behave like a spring: The hand controller deviation from its equilibrium position is proportional to the imposed contact force. Inspection of Fig. 4 reveals that $x = (S + GK)f$, where $S + GK$ represents the total sensitivity of the hand controller. The value of K must be chosen such that $S + GK$ becomes equal to the desired sensitivity while the system stability is guaranteed. Since G (shown in Fig. 7) is constant within its bandwidth, we choose K as a first-order transfer function [Eq. (8)] with a bandwidth larger than the bandwidth of G. This results in a constant overall sensitivity $S + GK$ within the bandwidth of G.

Figure 9 shows f vs x for various values of K_0 when the operator pushes the hand controller uniformly. In all cases the value of K_0 (the maximum value of K for all frequencies) was less than $1/H$, satisfying the stability condition in inequality (5). The slope of each plot in Fig. 9 represents the hand controller overall sensitivity or $S + GK$. Since S is small and G is unity within its bandwidth, the slope of each plot represents K_0.

B. Performance with High-Frequency Maneuvers

In another set of experiments, the operator maneuvers the hand controller irregularly (i.e., randomly). Figure 10 shows the history of the hand controller position x and the human force f as functions of time where $K_0 = 0.2$, satisfying the stability condition in inequality (5). Irregular maneuvers create high-and low-frequency components in the hand controller motion. Figure 11 shows the measured force f vs x where the slope of 0.2 implies that the desired sensitivity of $K_0 = 0.2$ has been achieved within the system bandwidth. Figures 12 and 13 are similar to Figs. 10 and 11; however, they are given for $K_0 = 0.1$. Inspection of the slope in Fig. 13 verifies that desired sensitivity of $K_0 = 0.1$ has been achieved within the system bandwidth.

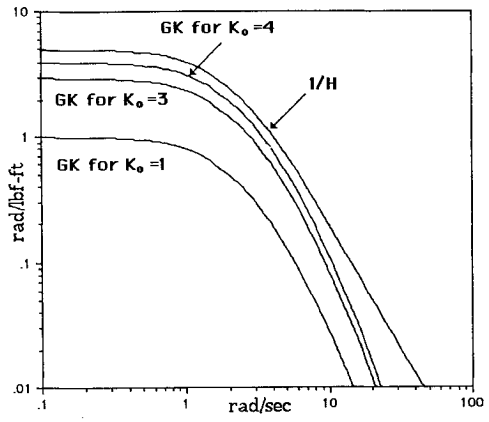

Fig. 14 For all values of $K_0 < 5$, $|GK| < |1/H|$ and satisfies stability condition of inequality (5).

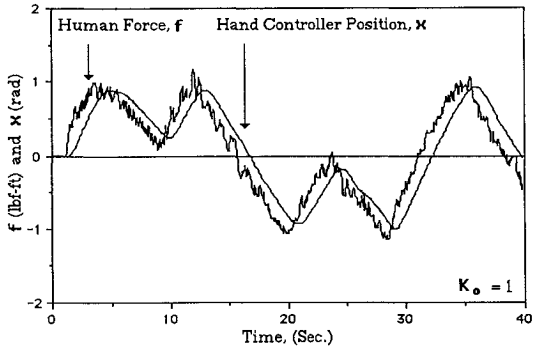

Fig. 15 Stable time history of human force f and hand controller position x.

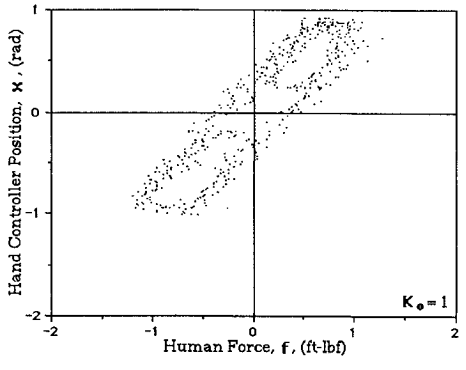

Fig. 16 Average slope of 1 reveals that $x = 1f$ for all frequencies within system bandwidth.

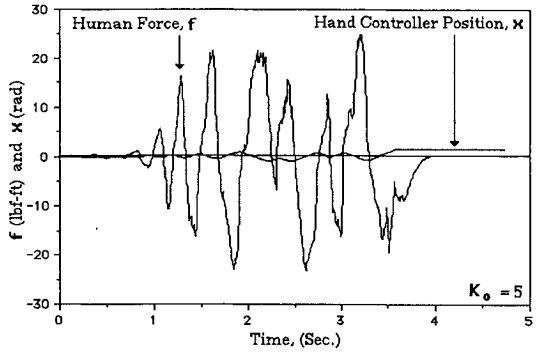

Fig. 17 Unstable time history of human force f and hand controller position x when the controller violates stability condition.

C. Stability Condition

A set of experiments was carried out to verify the stability condition. Here K was chosen to be

$$K = \frac{K_0}{(s/2 + 1)2}$$

Figure 14 shows GK for various values of K_0; it can be observed that for all values of $K_0 < 5$, $|GK| < |1/H|$, satisfying the stability condition [inequality (5)]. Figure 15 shows the system response (x and f) when $K_0 = 1$, satisfying the stability condition. Figure 16 shows the measured force f vs x where the slope of 1 implies that the desired sensitivity of $K_0 = 1$ has been achieved within the system bandwidth. Figure 17 shows a maneuver where $K_0 = 5$ violated the stability criterion, resulting in an unstable system.

VII. Conclusion

A control architecture has been given to develop compliancy in a hand controller. It has been shown that, for the stability of the hand controller and the human arm considered together as a single system, there must be some compliancy either in the hand controller or in the human arm. A single-degree-of-freedom powered hand controller has been built for theoretical and experimental verification of the hand controller dynamics. A set of experiments are given to verify the system performance and stability condition.

References

[1]Lippay, A. L., King, M., Kruk, R. V., and Morgan, M., "Helicopter Flight Control with One Hand," *Canadian Aeronautics and Space Journal*, Vol. 31, No. 4, 1985, pp. 20–23.

[2]Glusman, S. I., Landis, K. H., and Dabundo, C., "Handling Qualities Evaluation of the ADOCS Primary Flight Control System," *42nd Annual Forum of the American Helicopter Society,* American Helicopter Society, Washington, DC, 1986, pp. 56–62.

[3]Bruno, J. M., "Anthropomorphic Exoskeleton Dual Arm/Hand Telerobot Controller," *Proceedings of the IEEE International Workshop on Intelligent Robots and Systems* (Tokyo, Japan), Inst. of Electrical and Electronics Engineers, Piscataway, NJ, 1988, pp. 715, 717.

[4]Hollerbach, J. M., and Lokhorst, D. M., "Closed-Loop Kinematics Calibration of the RSI 6-DOF Hand Controller," *IEEE International Conference on Robotics and Automation* (Atlanta, GA), Inst. of Electrical and Electronics Engineers, Piscataway, NJ, 1993, pp. 142–148.

[5]Kazerooni, H., Tsay, T.-I., and Hollerbach, K., "A Controller Design Framework for Telerobotic Systems," *IEEE Control Systems Technology*, Vol. 1, No. 1, 1993, pp. 50–62.

[6]Hayati, S., Lee, T., Tso, K., Backes, P., and Lloyd, J., "A Testbed for a Unified Teleoperated-autonomous dual-arm robotic systems," *IEEE International Conference on Robotics and Automation* (Cincinnati, OH), Inst. of Electrical and Electronics Engineers, Piscataway, NJ, 1990, pp. 1090–1095.

[7]Anderson, R. J., and Spong, M. W., "Bilateral Control of Teleoperators with Time Delay," *IEEE Transactions on Automatic Control,* Vol. 34, No. 5, 1989, pp. 494–501.

[8]Bejczy, A. K., Bekey, G., and Lee, S. K., "Computer Control of Space Borne Teleoperators with Sensory Feedback," *IEEE Conference on Robotics and Automation*, Inst. of Electrical and Electronics Engineers, Piscataway, NJ, 1985, p. 205.

[9]Vertut, J., and Coiffet, M., *Teleoperators and Robotics*, Vol. 3A, Prentice-Hall, Englewood Cliffs, NJ, 1986.

[10]Kazerooni, H., and Guo, J., "Human Extenders," *ASME Journal of Dynamic Systems, Measurement and Control*, Vol. 115, 1993, pp. 190–281.

[11]Spong, M. W., and Vidyasagar, M., "Robust Nonlinear Control of Robot Manipulators," *Proceedings of the Twenty-Fourth IEEE Conference on Decision and Control* (Ft. Lauderdale, FL), Inst. of Electrical and Electronics Engineers, Piscataway, NJ, 1985, pp. 1767–1772.

[12]Stein, R. B., "What Muscles Variables Does the Nervous System Control in Limb Movements?" *Journal of the Behavioral and Brain Sciences*, Vol. 5, 1982, pp. 535–577.

[13]Berthoz, A., and Metral, S., "Behavior of Muscular Group Subjected to a Sinusoidal and Trapezoidal Variation of Force," *Journal of Applied Physiology*, Vol. 29, 1970, pp. 378–384.

[14]Lehtomaki, N. A., Sandell, N. R., and Athans, M., "Robustness Results in Linear-Quadratic Gaussian Based Multivariable Control Designs," *IEEE Transactions on Automatic Control*, Vol. AC-26, No. 1, 1981, pp. 75–92.

[15]Kazerooni, H., "Human-Robot Interaction via the Transfer of Power and Information Signals," *IEEE Transactions on Systems and Cybernetics,* Vol. 20, No. 2, 1990, pp. 450–463.